NOVEMBER 2018 M.Sc. in Electrical and Electronics Engineering EFGAN UĞUR

UNIVERSITY OF GAZİANTEP

GRADUATE SCHOOL OF

NATURAL & APPLIED SCIENCES

A SIMULATION STUDY ON AUTONOMOUS WHEELCHAIR CONTROL WITH VISUAL FEEDBACK FOR FOLLOWING STRAIGHT LINES

M. Sc. THESIS

IN

ELECTRICAL AND ELECTRONICS ENGINEERING

BY

EFGAN UĞUR

NOVEMBER 2018

A Simulation Study on Autonomous Wheelchair Control with Visual Feedback for Following Straight Lines

Electrical and Electronics Engineering

Master Thesis

Supervisor

Asst. Prof. Dr. Tolgay KARA

Efgan UĞUR

November 2018

REPUBLIC OF TURKEY
UNIVERSITY OF GAZİANTEP
GRADUATE SCHOOL OF NATURAL & APPLIED SCIENCES
ELECTRICAL-ELECTRONICS ENGINEERING

Name of the thesis: A Simulation Study on Autonomous Wheelchair Control with Visual Feedback for Following Straight Lines

Name of the student: Efgan UĞUR

Exam date: 27/11/2018

Approval of the Graduate School of Natural and Applied Sciences

Prof. Dr. A. Necmeddin YAZICI
Director

I certify that this thesis satisfies all the requirements as a thesis for the degree of Master of Science.

Prof. Dr. Ergun ERÇELEBİ
Head of Department

This is to certify that we have read this thesis and that in our consensus opinion it is fully adequate, in scope and quality, as a thesis for the degree of Master of Science.

Asst. Prof. Dr. Tolgay KARA
Supervisor

Examining Committee Members:	Signature
Prof. Dr. Ergun ERÇELEBİ	……..
Asst. Prof. Dr. K. Sercan BAYRAM	……..
Asst. Prof. Dr. Tolgay KARA	……..

I hereby declare that all information in this document has been obtained and presented in accordance with academic rules and ethical conduct. I also declare that, as required by these rules and conduct, I have fully cited and referenced all material and results that are not original to this work.

Efgan UĞUR

ABSTRACT

A SIMULATION STUDY ON AUTONOMOUS WHEELCHAIR CONTROL WITH VISUAL FEEDBACK FOR FOLLOWING STRAIGHT LINES

UĞUR, Efgan

M.Sc. in Electrical and Electronics Engineering

Supervisor: Asst. Prof. Dr. Tolgay KARA

November 2018

60 pages

Scope of the research is modeling, simulation and control design of an autonomous wheelchair with control purposes. Currently available electric wheelchairs fail in satisfying the needs of disabled people in many cases such as neuromuscular disabilities and reflex disabilities. Additionally, wheelchair outdoor navigation encounters high risk and serious challenges. The study aims to solve mobility problem of disabled people by adding visual information technology and efficient motion control and navigation design to standard electric wheelchair. Vision has proved to be the most versatile sensor for robotic applications, since it passively provides accurate and non-contact measurements of the environment with low cost. In this research, first the mathematical model of wheelchair dynamics is built in such a way that it describes the main characteristics and dynamical behavior of system. Then, vanishing point detection algorithm is applied. A computer simulation model is developed to observe the results of the study. Using the results of simulation tests, control algorithm is developed for efficient motor control. Linear displacement, position control, direction control and velocity of wheelchair are presented in the computer simulation. Motion control and tracking via visual feedback is achieved using a feedback control system with visual data collected from outdoor environment. The results show that the desired goals are achieved.

Key Words: Visual servoing, Smart wheelchair, Assistive robotics.

ÖZET

DÜZ ÇİZGİ TAKİBİ İÇİN GÖRSEL GERİ BESLEMELİ OTONOM TEKERLEKLİ SANDALYE KONTROLÜ ÜZERİNE BİR SİMULASYON ÇALIŞMASI

UĞUR, Efgan

Yüksek Lisans Tezi, Elektrik ve Elektronik Mühendisliği

Tez Yöneticisi: Dr. Öğr. Üyesi Tolgay KARA

Kasım 2018

60 sayfa

Bu araştırma, otonom bir tekerlekli sandalye sisteminin modellenmesi, simülasyonu ve kontrol tasarımını kapsamaktadır. Mevcut elektrikli tekerlekli sandalyeler, kas ve sinir hastalıkları olan veya reflekslerini kullanamayan engellilerin ihtiyaçlarını karşılamada başarısız olmaktadır. Ayrıca, tekerlekli sandalye kullanımında dış mekan navigasyonu, yüksek risk ve ciddi zorluklar içermektedir. Bu çalışma, standart elektrikli tekerlekli sandalyeye görüntü işleme teknolojisi, etkili hareket kontrolü ve navigasyon tasarımı ekleyerek engelli kişilerin hareketlilik sorununu çözmeyi amaçlamaktadır. Görsel alıcılar, pasif olarak doğru ve temassız ölçüm sağlamaları ve düşük maliyetleriyle robotik uygulamalar için en çok yönlü sensör olduğunu kanıtlamıştır. Bu araştırmada, öncelikle, tekerlekli sandalye dinamiğinin matematiksel modeli, sistemin temel özelliklerini ve dinamik davranışını tanımlayacak şekilde inşa edilmiştir. Ardından variş noktası belirleme algoritması uygulanmıştır. Çalışmanın sonuçlarını gözlemlemek için bir bilgisayar simülasyon modeli oluşturulmuştur. Simülasyon testlerinin sonuçlarını kullanarak, motor kontrolü için kontrol algoritması geliştirilmiştir. Tekerlekli sandalyenin lineer yer değiştirme, konum, yön ve hız kontrolü bilgisayar simülasyonunda sunulmaktadır. Hareket kontrolü ve görsel geri besleme yoluyla izleme de dış ortamdan toplanan verilerle geri bildirim kontrol sistemi kullanılarak elde edilir. Sonuçlar istenilen hedeflere ulaşıldığını göstermektedir.

Anahtar Kelimeler: Görsel servolama, Akıllı tekerlekli sandalye, Yardımcı robotlar.

"To my family"

ACKNOWLEDGEMETS

I would like to express my deepest gratitude to my supervisor Asst. Prof. Dr. Tolgay KARA for his guidance, advice, criticism, encouragements and insight throughout this study.

I would like to thank Dr. Abdulhafez ABDULHAFEZ, without whom this thesis would not be possible, for including me in his research project and guiding me with his valuable advice.

This work is supported by The Scientific and Technological Research Council of Turkey (TUBİTAK), through project 117E173.

TABLE OF CONTENTS

Page

LIST OF TABLES

Page

LIST OF FIGURES

Page

LIST OF SYMBOLS / ABBREVIATIONS

IBVS	Image-based visual servoing
GPS	Global positioning system
HOG	Histogram of Gaussian
SIFT	Scale-invariant feature transform
SURF	Speeded-up robust features
SQL	Structured Query Language
WI-SURF	Whole image scale-invariant feature transform
ROS	Robot operating system
UVSS	Ubiquitous visual sensor system
DC	Direct current
PW	Power wheelchair
EMF	Electromagnetomotive force
ATEKS	Akıllı Tekerlekli Sandalye
RADHAR	Robotic Adaptation to Humans Adapting to Robots
INS	Inertial Navigation System
LIDAR	Laser Imaging Detection and Ranging
$\boldsymbol{E_a}$	Motor armature voltage
$\boldsymbol{E_b}$	Motor electromagnetomotive force
$\boldsymbol{F_1, F_2}$	Wheelchair driving forces
$\boldsymbol{F_i}$	Driving force of wheel i
$\boldsymbol{F_3, F_4, F_7, F_8}$	Caster reaction forces
$\boldsymbol{F_{r1}, F_{r2}, F_{r3}, F_{r4}}$	Resistive forces
$\boldsymbol{F_{T1}, F_{T2}, F_{T3}, F_{T4}}$	Sliding wheel forces
G	Worm gear reduction factor

$\boldsymbol{i_a}$	Motor armature current
$\boldsymbol{I_{c1}, I_{c2}}$	Moment of inertia of the caster
$\boldsymbol{I_0}$	Moment of inertia of the frame
$\boldsymbol{J_m}$	Motor shaft inertia
$\boldsymbol{K_T}$	Motor torque constant
$\boldsymbol{K_v}$	Motor velocity constant
$\boldsymbol{L_a}$	Motor armature inductance
G	Gradient
G_x, G_y	Gradient components
$\propto$	The angle of orientation of the edge
P_1, P_2, P_3, P_4, P_5	Pseudo – convolution kernels
P_6, P_7, P_8, P_9	Pseudo – convolution kernels

CHAPTER 1

INTRODUCTION

Visual navigation in outdoor environments faces several challenges. These are, for one example, urban structure obstacles like sidewalks, trees, sign boards and street furniture. Another challenge is that outdoor environments suffer from high change in appearance and illumination from time to time in the day, and from season to season in a year. This is in addition to the dynamic elements like pedestrians, vehicles. Indeed, visual features need to be carefully selected and extracted, and an efficient motion control design is required. This research considers visual wheelchair navigation using only vision sensors in outdoor environments. The list of original contributions includes algorithms, methods and visual control designs. These contributions are detailed in the coming chapters.

Theoretically, navigation using visual memory utilizes an image space path planning in the visual memory; the chair is physically following this path utilizing qualitative image-based visual servoing (IBVS). The path is defined as a set of intermediate images while the task of the IBVS controller is to drive the chair through places which are represented using these intermediate images. The task is designed to completion by proposing a visual controller that utilizes the well common IBVS along with robust features extraction methods to be used in the control law. These features are the vanishing point which is appeared due to straight lines in the urban environment, and the line of gravity of yellow color tactile path marker which will be robustly detected and tracked. The robustness of features extraction is considered here with respect to occlusion and to illumination variances in outdoor environments.

The thesis has strong social and economic impact since it provides supports for disables to increase their mobility. The work provides vision based cheaper and efficient replacement of other systems that use multiple expensive sensory for wheelchair system

1.1 Motivation

Social support to disabled persons focuses on increasing their mobility and interaction with the environment and the society. Electrical wheelchairs play an essential role in boosting the mobility of physically disabled individuals in their environment. Typically, environments can be categorized as indoor and outdoor environments. Challenges for wheelchair navigation in indoor environments are limited space, high probability of collision, and the impossible yet stair climbing. On the other hand, interacting with people, vehicles, and obstacles in urban structures are the challenges for outdoor environments. Urban structures are like sidewalks, street signposts, poles, bus-stops cabins, and street furniture. Indeed, wheelchair outdoor navigation encounters high risk and serious challenges. Several previous works attempted to solve both indoor and outdoor navigation problems as cited in the following sections. These works build multi-sensor systems using different sensory techniques like laser and ultrasonic range finder, proximity sensors, etc. This thesis proposes motion control and tracking via visual feedback is also achieved using a feedback control system with visual data collected from only vision sensor .

1.2 Literature Review

Recent appearance-based navigation methods in outdoor environments focus on localization from image matching and alignment, and use features that are invariant to appearance changes over seasons and cross day to night time. For example, the work presented performs localization via matching of sequence of image information[1]. Technically, a graph of network flow is exploited along with GPS (Global Positioning System) prior information to perform the localization task. The methods proposed in the work have shown robust performance against the appearance changes[2]. It uses Histogram of Gaussian (HOG) features and deeply learned features. However, it is shown in another work that these methods cannot cope with the situation of dynamic and crowded environments[3]. Instead, a further learning method is used to learn only useful and relevant SIFT (Scale-invariant feature transform) features to solve the localization problem. Another type of feature, color histogram, is used in but it was not tested in outdoor environments[4]. A sequence of binary features has been proposed and it is that an efficient but low cost localization can be achieved using binary descriptors of an image sequences[5]. It is worth to note here that recent success in outdoor navigation has been feasible due to proposal of modern features. Navigation

algorithm uses the state of the art Histogram of Gradients (HOG) features, which was proved to be hardly discriminating over temporal environment changes [1]. HOG features outperform traditional features like SIFT and SURF (Speeded-up robust features) in different aspects, particularly time complexity and discriminability.

It is presented an outdoor scalable appearance-based navigation framework[6]. This framework is based on learning the environment and building a map using recorded sequence of images, i.e. visual memory. The learning motion is under human control. However, the learning is high-level and requires the storage of set of key-images in the form of visual memory. In these frameworks, an IBVS is employed to drive the robot between every two successive images. The framework is tested on 200 meters long mostly straight path while neither dynamic elements nor variable appearance are being considered. Even though the system was successfully able to follow the learned path, this system requires a priori knowledge of the environment. More recently, a research proposed a similar navigation system for a mobile robot, but with laser-based collision avoidance[7]. However, this system is additionally equipped with active pan and tilt camera to maintain the visibility of the path along with an on-board laser range finder. It is worth to note that this work was the first to tackle the obstacle avoidance problem in appearance-based navigation framework, but it is using laser sensor integrated with the active vision-based controller. All works cited in this paragraph consider features that have SIFT-type descriptors and Harris point detectors. They are demonstrated in outdoor but with same appearance conditions where there is no change in illumination. In addition, these works consider small-scale environment.

Since our proposal considers larger environment, image retrieval method from large scale environment is required. We propose to use HOG features in visual memory based navigation framework utilizing the image space histogram of gradients to achieve a novel qualitative HOG-based visual control law.

1.2.1 Visual Features Selection

Recent successful attempts in visual outdoor navigation are due to two main factors. The first is the selected features that are invariant to changes in illumination and lightening conditions like HOG in a work [1], SIFT features in [9], and whole image SURF features in [10]. Second factor is the assumptions that dynamic elements are not considerably available in the scene [6,2,7]. If a priori knowledge is available, a

learning method can be utilized to learn and filter the dynamics out [3]. Our problem is challenging and new because it considers outdoor environment. In particular, it is city urban streets and walking passages, which is structured but fully equipped with pedestrians. Features like SIFT, SURF, whole image SURF (WI-SURF), and Histogram of Gradients (HoG) are reported to achieve quite good for visual localization and are considered to be used. It is well common in the literature that SIFT and SURF features are the most popular descriptors in the vision community. However, whole image SURF (WI-SURF) and histogram of Gradient HoG are achieving quite better for localization in outdoor environment that show high changes in appearance due to illumination effects, like day to night time or across seasons[10].

1.2.2 Vanishing Point Estimation

Vanishing points are an image plane points (xf ,yf) defined as the convergence points of images of all parallel 3D (3-dimension) line. It was proved in the literature that there are at most three vanishing points each of which is attached to one 3D space direction [11]. Even though we are working with outdoor environment path following, we assume that the environment is man-made hence vanishing points are available and they can be easily extracted. The computer vision literature is rich with works on the problem of finding vanishing points in an image [12-16]. In addition, several applications of vanishing points were proposed in robotics community [17-20], but they were very simple methods and rely on well-structured but non practical environment. Most of the vanishing point detection methods use Gaussian sphere [12,21]. Gaussian sphere is a 2D (2-dimension) accumulator array each of its elements contains a list of line segments and the count of those segments. Of course, these line segments are detected from the current image using typical image edge detectors.

1.2.3 Wheelchair Control and Navigation

Recent advances in smart technology and robotics facilitate new designs that help improving the way in which disabled people live. The advances can enhance the electric-powered wheelchair into a “Smart Wheelchair” via intelligent sensory and control techniques. Works on intelligent wheelchairs usually focus on boosting the safety level. Examples are works reported in [22-25]. ATEKS (Akıllı Tekerlekli Sanadalye) is one of the recent works in Turkey on intelligent and smart wheelchair [26]. The work is the most recent work that tackles the outdoor wheelchair

problem[27]. The European RADHAR (Robotic Adaptation to Humans Adapting to Robots) project targets the semi-autonomous navigation of wheelchair[23]. It is basically a navigation assistance framework for fusing environment and user perception, and for taking safe robot navigation actions based on the estimated robot task from uncertain driver signals, with an ability to take navigation decisions at 5 Hz rates or higher. The work proposed in SYSIASS project employs a laser range finder with classical linear controller, i.e. PID controller, to perform the task of doorway passing[24,25]. The SYSIASS project has designed a research oriented platform with the aim of connecting technologies to research on collision avoidance and Assistive Technologies for powered wheelchairs. Two types of ranging sensors, ultrasonic (US) and infrared (IR) are used to mutually perceive the environment fields grouped on the wheelchair together by location. Sensors are controlled by a dedicated ATmega328 microprocessor board (Arduino Mini). It is a multi-sensor mobile platform presented as indoor navigation for smart wheelchair. The system utilizes 10 ultrasonic sensors, indoor positioning system, and Kinect as range finder. In ATEKS, fuzzy control system is implemented on the robot operating system to handle the goal reaching and obstacle avoidance tasks. In a study, they have modified the mobile robot ATEKS, which is an intelligent wheelchair, by introducing three fuzzy inference systems to realize goal reaching, obstacle avoidance and a controller for combined behavior selection[26]. Designed fuzzy control system has been implemented on Robot Operating System (ROS) under Ubuntu 12.04 operating system and tested under Gazebo simulation platform. Simulation results verified faithful behavior outputs of ATEKS. The work proposed in another research uses sonar data to design stable control law for mobile robot[28]. This mobile robot performs the tasks of corridor following and wall following. Visual navigation algorithms are presented to achieve the corridor navigation task[29]. These algorithms use optical flow and the vanishing point at which walls and floor lines meet. Hybrid control algorithm that employs laser and vision for dynamic obstacle avoidance and path planning was proposed [30].

The work presents a new navigation and control of wheelchair by utilizing global tracking and servoing techniques, in contrast to the conventional on-board local sensors which provide local environment map[31]. They call it Ubiquitous Visual Sensor System (UVSS). It can perform tasks like navigation, control, and obstacle avoidance. However, the navigation system is presented as network service since the

visual sensors are distributed sensory systems. The system includes mainly real-time wheelchair tracking module and networked control and communication module. The proposed system is verified and experimented in a limited indoor environment only. The work proposes a human-in-the-loop control structure with real-time assistive levels[32]. One of these levels offers improved dynamic modeling and three of these levels offer unique and novel real-time solutions for: collision avoidance, localization and waypoint identification, and assistive trajectory generation. This architecture and these assistive functions always allow the user to remain fully in control of any motion of the powered wheelchair, shown in a series of experiments. The work shows that in order to provide a safe robust assistive power wheelchair there will be a need to employ multiple sensor types to ensure that obstacles are not overlooked or incorrect distances were avoided. However, it was claimed that combining multiple sensor data can be quite complex. A unified shared control framework which is able to smoothly correct the trajectory of the electrical wheelchair is proposed [33]. Clinical validation is also performed on the proposed architecture. The system integrates the manual control with sensor-based constraints by means of a dedicated optimization strategy. This assistive tool is shown to be intuitive and robust as it respects the user intention, and it does not alter perception while reducing the number of collisions in case of hazardous maneuvers or in crowded environments. These proposals that are mentioned above are multi-sensor systems. They do not consider outdoor challenges in large-scale environments as well. In contrast to these systems, we propose to utilize visual tracking and servoing platform to achieve outdoor visual navigation and control along with obstacle avoidance consideration. Most recent similar work is the one presented in [27]. It presents a method for development of smart wheelchair navigation system in urban environments. The system consists of two main parts: a mapping module that work offline on building a map of the environment from data acquired by 3D vision sensors. The mapping module provides the mapping service to the wheelchair navigation system considering it as a client. The navigation system itself uses GPS/INS (Inertial navigation system), 3D LIDAR (Laser Imaging Detection and Ranging) and 3D vision sensors for perception and localization in the environment. The system demonstrates autonomous navigation in urban environment for long over 12 km. The main difference from our proposal is that we do not plan to use 3D vision sensor due to its high cost, we plan to use only 2D visual but cheap cameras as well. In addition,

this work uses luxury and high end GPS/INS for accurate localization while we aim at obtaining high localization accuracy from visual memory only.

Considering that all of the works which are mentioned above are multi-sensor and distributed architecture systems, it is worth to mention that the most recent work is the only pure vision system that addresses the problem of indoor wheelchair corridor following[34]. It utilizes a single-architecture system equipped with three monocular cameras to achieve several tasks like corridor following and doorway passing in an indoor environment. This work is dedicated for indoor navigation using semi-autonomous scheme. Geometric features like the vanishing point and line features (the wall edges and the door edges) are extracted and used in the visual servoing control law to achieve the considered task. However, the methodology cannot be applied for outdoor navigation because of several challenges[34]. For example, visual occlusion due to dynamic elements like walking people, illumination changes make extraction of geometric feature is unrealizable, etc.

Recalling that our aim is to perform only-vision outdoor navigation, several challenges can be stated comparing to the previous works on robot in general and wheelchair navigation: (i) selecting visual features from the urban environment that are suitable for the navigation task and robust to environment changes and its dynamic aspects, and (ii) designing the navigation and control algorithm that is robust to loss of data due to dynamic aspects of the environment. One recent work attempts on the classification of urban terrain to four classes like grass, sidewalk, street, or unknown area[35]. Again, the system is not purely vision system, but it uses a 3D camera which is provided with range sensor. They were motivated by the conclusion given in the work which states that geometric features alone are not sufficient for robust navigation in urban environments[36]. Consequently, traditional geometric map-based navigation methods will not work here. Moreover, outdoor navigation is difficult in case of changes in appearance and illumination.

1.3 Problem Statement and Contribution of Thesis

As shown in previous section, all outdoor wheelchair navigation systems are multi-sensor systems that employ combination of vision with laser and sonar range finders for navigation tasks. This research accomplishes the tasks by using only vision sensors.

Of course the advantage of vision only sensory system is that vision sensors are low cost sensors. The cost of high performance GPS/INS or LIDAR sensory systems is in average 10,000 USD which is obviously impossible in smart powered wheelchair system. Out of the shelf low cost vision sensors can be employed in designing the required control system easily.

In conclusion, the goal which is tracking via visual feedback in outdoor environments are solved using image-based visual servo control. It is a new combination of selected features with a new control design.

1.4 Organization of Thesis

The current chapter gives an overview about autonomous wheelchair system's control problem and proposed different solutions. The mathematical model of the autonomous wheelchair system is built in Chapter II. Chapter III presents control system design and simulation of the autonomous wheelchair. Linear displacement, position control, direction control and velocity of wheelchair are presented in the computer simulation results and effect of disturbances, influences of rider mass are shown by the simulated system in Chapter IV. Also, this chapter includes visual feedback control. In the end, discussion and conclusion of thesis are stated in Chapter V.

CHAPTER 2

MATHEMATICAL MODEL OF ELECTRIC WHEELCHAIR

2.1 Introduction

The electric wheelchair is a unique vehicle which possesses characteristics that are very different from those of automobiles or other forms of transportation. Figure 2.1 is one of the example of typical model. Rear wheels have propulsion systems and they have seperately DC electric motors. Two front casters wheels are passive elements that support part of the wheelchair weight and facilitate turning by changing their orientation as the wheelchair turns. Knowing the forces and torques, one can figure out how a mechanism will move. So, dynamic equations of rear wheels are more important because of motors.

Figure 2.1 Typical electric wheelchair

The dynamics of the wheelchair system are described by the mathematical model in order to develop efficient control system for motion control and navigation. The model includes many factors which effect the motion of the wheelchair. Wheelchair driving forces, frictional forces, sliding wheel forces and caster reaction forces are some of

them. Additionally, there are minor factors such as rolling resistance, axle friction and air drag. The model developed in this section relies on the standard mathematical relations available in literature, which provide a stepping-stone for wheelchair designers by incorporating analytical modeling [37-38]. The schematic diagram of the top view of a typical wheelcair is presented in Cartesian plane in Figure 2.2. An ideal wheelchair caster structure is also presented in Figure 2.3.

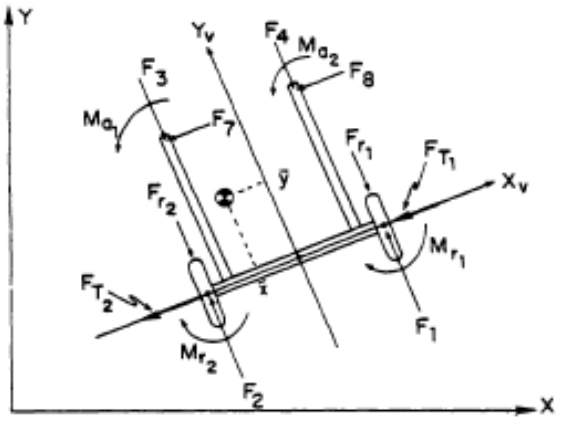

Figure 2.2 Rigid body of wheelchair frame and rider in its inertial reference frame[37].

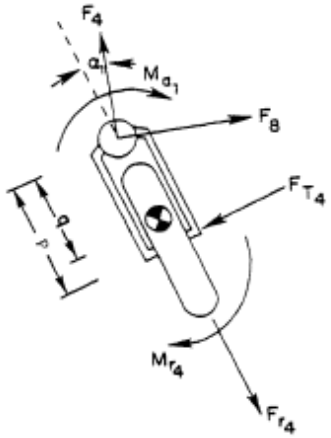

Figure 2.3 Schematic diagram of ideal wheelchair caster [37].

2.2 Dynamic Equations of Motion

The mathematical relations for the motion of the wheelcahair can be obtained using force balance equation in Newtonian mechanics as follows [37]:

$$\frac{M_F R}{2}\left(\left(1+\frac{2\bar{x}}{R_r}\right)\ddot{\theta}_1+\left(1-\frac{2\bar{x}}{R_r}\right)\ddot{\theta}_2\right)=F_1+F_2-F_{r3}\cos\alpha_2-F_{r4}\cos\alpha_1-F_{T3}\sin\alpha_2-F_{T4}\sin\alpha_1-F_{r1}-F_{r2} \quad (2.1)$$

$$\frac{R}{R_r}\left(I_0 + M_F\left(\bar{x}^2 + \frac{2\bar{x}}{R_r} + \bar{y}^2\right)\right)\ddot{\theta}_1 + \frac{R}{R_r}\left(-I_0 + M_F\left(-\bar{x}^2 + \frac{2\bar{x}}{R_r} - \bar{y}^2\right)\right)\ddot{\theta}_2 = (F_1 - F_2)\frac{R_r}{2} + \cos\alpha_1\left(R_L F_{T4} - \frac{R_F}{2}F_{r4}\right) + \cos\alpha_2\left(\frac{R_F}{2}F_{r3} - R_L F_{T3}\right) + M_{a1} + M_{a2} - \sin\alpha_1\left(R_L F_{r4} + \frac{R_F}{2}F_{T4}\right) - \sin\alpha_2\left(R_L F_{r3} + \frac{R_F}{2}F_{T3}\right) - M_{r1} - M_{r2} + \frac{R_r}{2}(F_{r2} - F_{r1}) \quad (2.2)$$

The mathematical relations presented in equation (2.1) and equation (2.2) describe two of the four equations of motion. The other equations involve the rotational degrees of freedom of the two casters. Referring to Figure 2.3 and the D'Alembert's principle, assuming the D'Alembert forces to be negligible, and taking moments about the point at which the caster connects to the frame results in the following equations [37]:

$$I_{c1}\ddot{a}_1 = -pF_{T4} - M_{r4} - M_{a1} \quad (2.3)$$

$$I_{c2}\ddot{a}_2 = -pF_{T3} - M_{r3} - M_{a2} \quad (2.4)$$

Equations from (2.1) to (2.4) constitute the equations of motion of the wheelchair system. The model of wheelchair mechanics presented in equatios from (2.1) to (2.4) should be combined with the electrical model for a complete control-oriented model of PW (Power Wheelchair) dynamics. The structure of the Direct Current (DC) motor system driving the motion of the wheelchair is presented in Figure 2.4, which also represents the link between electrical and mechanical parts of the electromechanics involved in the system. When the armature circuit is considered only, the following equation is obtained [39].

$$E_a = R_a i_a + L_a\frac{di_a}{dt} + E_b \quad (2.5)$$

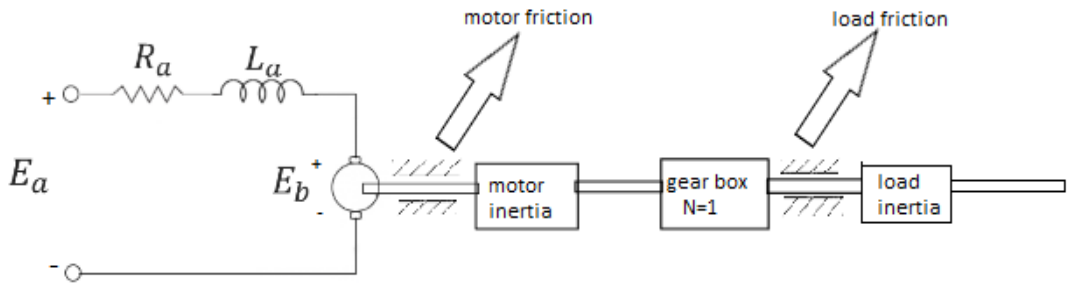

Figure 2.4 Model of the wheelchair DC motor

The following series of mathematical relations describe how the mechanical and electrical parts of the wheelchair system can be combined together [37]. The back Electromagnetomotive Force (EMF) can be directly related to motor speed which in turn is directly related to wheel speed as follows.

$$E_b = K_v \dot{\theta}_m = K_v \frac{GR_p}{R_m} \dot{\theta}_i \tag{2.6}$$

This allows equation (2.6) to be written as

$$\frac{di_a}{dt} = \frac{1}{L_a}\left(E_a - R_a i_a - K_v \frac{GR_p}{R_m} \dot{\theta}_i\right) \tag{2.7}$$

Equation (2.7) gives the resulting current, which is used to determine driving forces in equation. (2.8).

$$F_i = \frac{GR_p}{RR_m}\left(K_T i_a - J_m \ddot{\theta}_m - \beta_m \dot{\theta}_m\right) \tag{2.8}$$

Also, effect of rider mass is analyzed in the simulations by using the following formulas:

$$N_1 = \frac{W_T}{2}\left(1 + \frac{2\bar{x}}{R_r}\right)\left(1 - \frac{\bar{y}}{R_L}\right) \tag{2.9}$$

$$N_1 = \frac{W_T}{2}\left(1 - \frac{2\bar{x}}{R_r}\right)\left(1 - \frac{\bar{y}}{R_L}\right) \tag{2.10}$$

2.3 System Parameters

Some of the parameters in equations of motion are known or can be found easily. For instance, mass of body and wheel are measurable. On the other hand, inertia of body and motor parameters are found experimentally. Mass of body and wheel are measured easily, for instance. On the other hand, inertia of wheel and motor parameters are found experimentally.

E_a is obtained from the motor datasheet as 24 Volts. Resistance of motor is measured via a multimeter. It is determined as 1.4 Ω, approximately. It is assumed that spring constant of motor (k) is negligible.

An encoder is built in order to determine back EMF constant of motor. It is assumed that right and left motors have same characteristics, so experiments are only performed on one motor. Encoder is mounted on the wheel which is shown in the Figure 2.5. This experiment results is referenced the work[40].

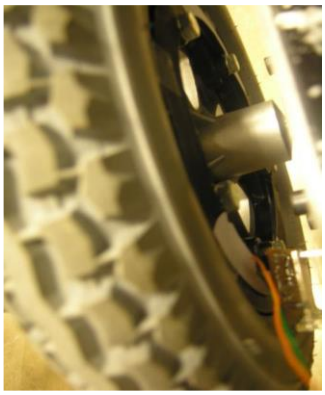

Figure 2.5 Encoder

The period of pulses are observed as 240 msec. at the maximum speed via oscilloscope. This means 480 msec. for one revolution. It gave 125 rpm or 13.09 rad./sec. for the output shaft. Figure 2.6 shows experimental setup.

Back EMF constant K_v and torque constant K_T are calculated by using the following equations (2.11),(2.12) and (2.13)

$$E_a - R_a i_a - L_a \frac{di_a}{dt} - E_b = 0$$
(2.11)

which is the equation from Kirchhoff's law. Back EMF voltage, E_b is related to armature velocity as:

$$E_b = K_v \dot{\theta}_m$$
(2.12)

Equation (2.13) is derived using (2.11) and (2.12) as:

$$E_a - R_a i_a = K_v \dot{\theta_m}$$
(2.13)

K_v is found as 0.05 V/rad/sec. The parameters are related to motor shaft, so velocity of output shaft was converted to velocity of motor shaft by multiplying gear ratio. It is assumed that motor torque constant, K_T has same magnitude with K_v.

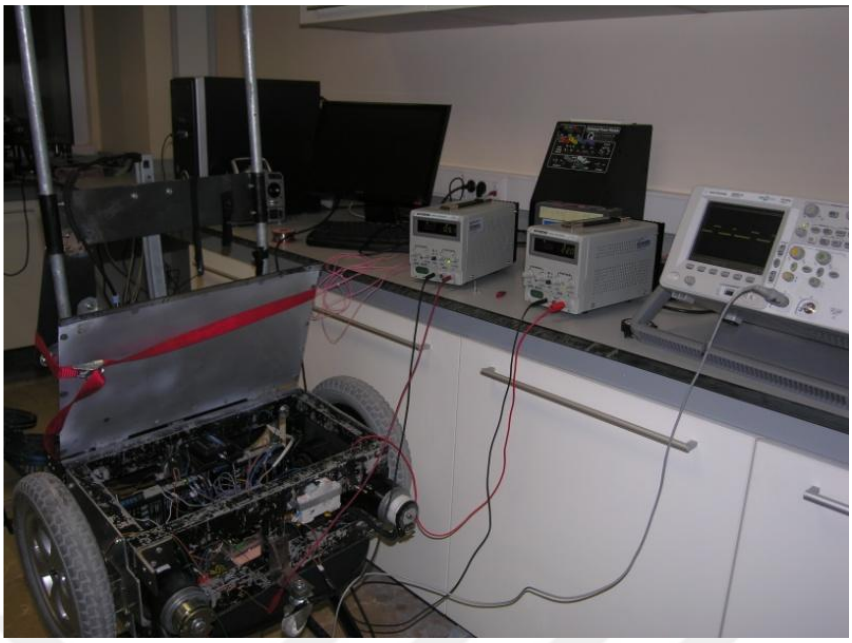

Figure 2.6 Back EMF constant experimental setup

It is assumed that motor torque constant K_T has same magnitude with K_v.

$$J_T = J_W + J_m + J_s \tag{2.14}$$

Because of motor inertia J_m and shaft inertia J_s have negligible values in comparison with wheel inertia J_W, total inertia is approximately equal to inertia of wheel. ($J_T \cong J_W$).

Inertia of the wheel is related to length of wheel shaft L_w, mass of the wheel m_w, radius R_w, gravity g and natural frequency. Then the equation is derived as follows:

$$J_W = \left[\frac{T}{2\pi}\right]^2 \frac{m_w g R_w^2}{L_w} \tag{2.15}$$

Table 2.1 Parameters for wheel inertia test

Length L_w	1.67 m
Radius R_w	0.2 m
Mass m_w	2.08 kg
Gravity g	9.8 m/s^2
Period T	1.45 s

These parameters are used in equation (2.15) and inertia of wheel is calculated as 0.0166 kg.m^2. By the combination of equations between the (2.1) and (2.15), mathematical model for the motion of chassis of the chair is obtained for computer simulation [41]

CHAPTER 3

SIMULATION MODEL

3.1 Introduction

Modeling and simulation of dynamic systems solves many real-world problems safely and efficiently. It provides an important method of analysis which is easily verified, communicated, and understood. Across industries and disciplines, simulation models provide valuable solutions by giving clear insights into complex systems.

The mathematical model of PW dynamics, which is made up of the mechanical and electrical parts has been presented in previous chapter. The control objective that involves motion control for the navigation of an autonomous wheelchair system requires this mathematical model to be presented and simulated in input-output form with control purposes.

3.2 Block Diagram

The block diagram of a proper feedback scheme for the control of the plant, which is the PW for our case, is presented in Figure 3.1. The block diagram is a graphical representation of the DC motors of the wheelchair system – it provides a functional view of a system. In this thesis, block diagram is constructed because control flow is important and graphical representation is often easier to understand than a textual representation. The electrical representation of DC motor is used here which is shown in Figure 2.4. It can be represented by a voltage source (E_a) across the coil of the armature. The electrical equivalent of the armature coil can be described by an inductance (L_a) in series with a resistance (R_a) in series with an induced voltage (E_b) which opposes the voltage source. The induced voltage is generated by the rotation of the electrical coil through the fixed flux lines of the permanent magnets. This voltage is often referred to as the back EMF.

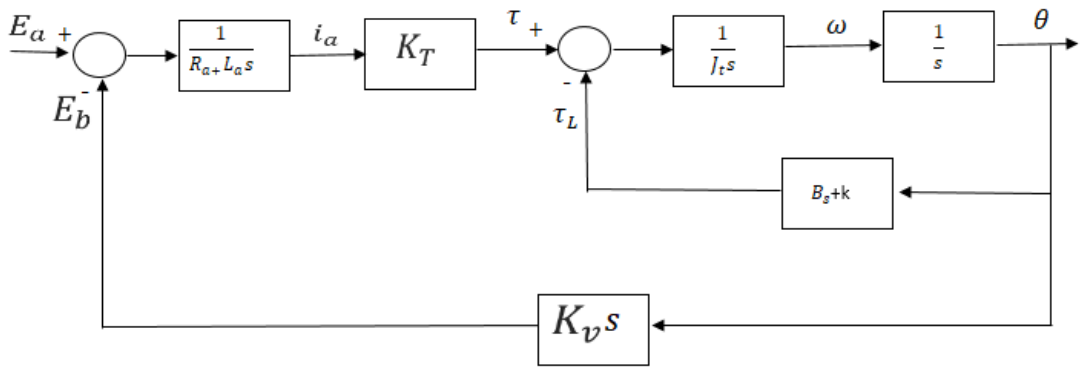

Figure 3.1 Block diagram of DC motor of the wheelchair

The model involves one outer feedback loop of the controller, and one inner loop that is inherent due to self-regulatory nature of the DC motor involved which is shown in Figure 3.2.

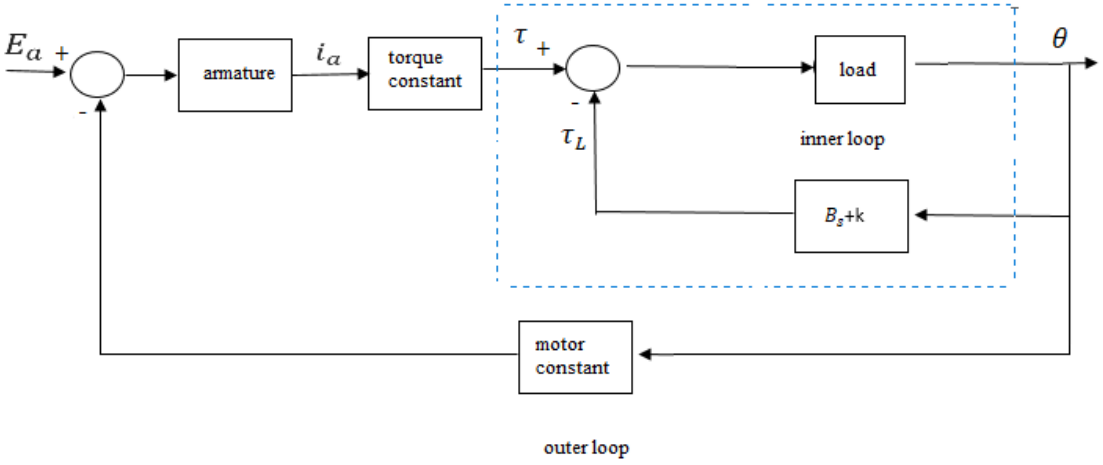

Figure 3.2 Inner loop and outer loop of block diagram

3.3 Methodology for vanishing point

Sobel which is a popular edge detection algorithm is considered in this thesis. The Sobel method uses the derivative approximation to find edges. Therefore, it returns edges at those points where the gradient of the considered image is maximum. The Sobel operator performs a 2-D spatial gradient measurement on images. It uses a pair of horizontal and vertical gradient matrices whose dimensions are 3×3 for edge detection operations.

Using computers to do image processing has two objectives: First, create more suitable images for people to observe and identify. Second, we wish that computers can automatically recognize and understand images. The edge of an image is the most basic

features of the image. It contains a wealth of internal information of the image. Therefore, edge detection is one of the key research works in image processing.

- Edges are significant local changes of intensity in an image.

- Edges typically occur on the boundary between two different regions in an image.

• Goal of edge detection

- Produce a line drawing of a scene from an image of that scene.

- Important features can be extracted from the edges of an image (e.g., corners, lines, curves).

- These features are used by higher-level computer vision algorithms (e.g., recognition).

The Sobel operator performs a 2-D spatial gradient measurement on an image and emphasizes regions of high spatial gradient that correspond to edges. Typically it is used

to find the approximate absolute gradient magnitude at each point in an input greyscale image. Compared to other edge operator, Sobel has two main advantages:

1. Since the introduction of the average factor, it has some smoothing effect to the random noise of the image.

2. Because it is the differential of two rows or two columns, so the elements of the edge on both sides has been enhanced, so that the edge seems thick and bright.[42]

In theory at least, the operator consists of a pair of 3×3 convolution kernels as shown in Figure 3.3. One kernel is simply the other rotated by 90°. This is very similar to the Roberts Cross operator.

-1	0	+1
-2	0	+2
-1	0	+1

G_x

+1	+2	+1
0	0	0
-1	-2	-1

G_y

Figure 3.3 Sobel convolution kernels

These kernels are designed to respond maximally to edges running vertically and horizontally relative to the pixel grid, one kernel for each of the two perpendicular orientations. The kernels can be applied separately to the input image, to produce separate measurements of the gradient component in each orientation (call these G_x and G_y). These can then be combined together to find the absolute magnitude of the gradient at each point and the orientation of that gradient. The gradient magnitude is given by:

$$|G| = \sqrt{G_x^2 + G_y^2} \tag{3.1}$$

Typically, an approximate magnitude is computed using:

$$|G| = |G_x| + |G_y| \tag{3.2}$$

which is much faster to compute.

The angle of orientation of the edge (relative to the pixel grid) giving rise to the spatial gradient is given by:

$$\propto = \arctan(\frac{G_y}{G_x}) \tag{3.3}$$

In this case, orientation 0 is taken to mean that the direction of maximum contrast from black to white runs from left to right on the image, and other angles are measured anti-clockwise from this.

Often, this absolute magnitude is the only output the user sees the two components of the gradient are conveniently computed and added in a single pass over the input image using the pseudo-convolution operator shown in Figure 3.4. [43]

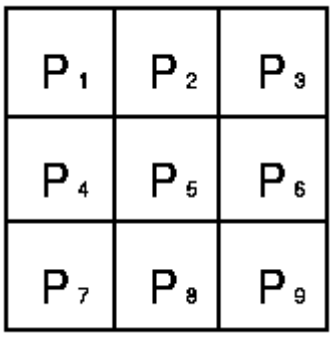

Figure 3.4 Pseudo-convolution kernels

Pseudo-convolution kernels is used to quickly compute approximate gradient magnitude.

Using this kernel the approximate magnitude is given by:

$$|G| = |(P_1 + 2 * P_2 + P_3) - (P_7 + 2 * P_8 + P_9| + |(P_3 + 2 * P_6 + P_9) - (P_1 + 2 * P_4 + P_7| \quad (3.4)$$

To find the vanishing point, firstly program finds the straight lines on the images. Then, the program sets angular variation evoluation value to the points on straight lines. Lastly, program sets the vanishing point. As shown in the Figure 3.5 red lines shows the straight lines and red point shows the vanishing point. And Figure 3.5 is example of vanishing point for outdoor environment. The method is used also corridor following by taking the straight lines which can be seen in the Figure 3.6. and the Figure 3.6 represents example of vanishing point for indoor environment. The methodology is used for as lane keeping assist on the cars by detecting the lanes which on the roads. It can be seen as one of the example in the Figure 3.7.

Figure 3.5 Vanishing point in outdoor environment

Figure 3.6 Vanishing point in indoor environment

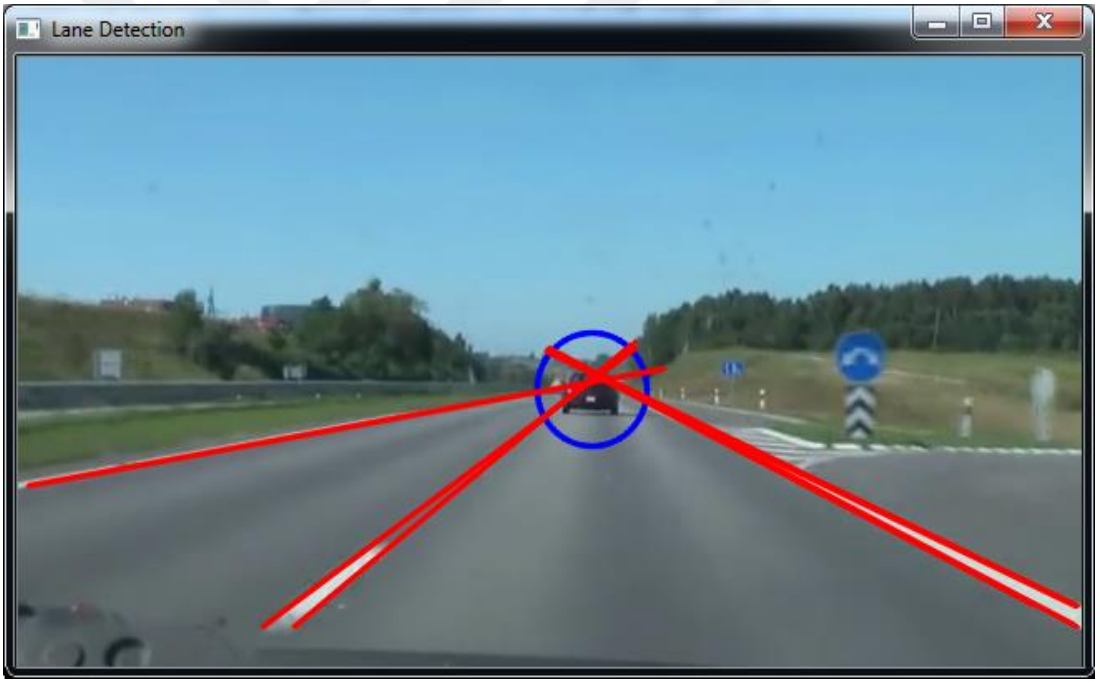

Figure 3.7 Vanishing point with lane detection

3.3.1 Algorithm for the system

Step 1: Determine first position.

Step 2: Find the vanishing point.

Step 3: Check line position.

Step 4: If they are not equal apply control action. Else go step 5.

Step 5: Go to vanishing point.

The steps which are on the above represents the algorithm of the wheelchair visual feedback control system. Firstly, determining the coordinate for wheelchair in idle position. Then, vanishing point is found by the code. After that, line position is checked continously and if there is any changes control action is applied. So, control of autonomous wheelchair is performed.

3.3.2 Flow chart of the system

The flowchart of the system is in the Figure 3.8. This process has feedback mechanism inside of the algorithm. The algorithm is constructed to the targeted position and this is provided by controlling the left and right motor. Motion control algorithm will be explained in the coming chapters.

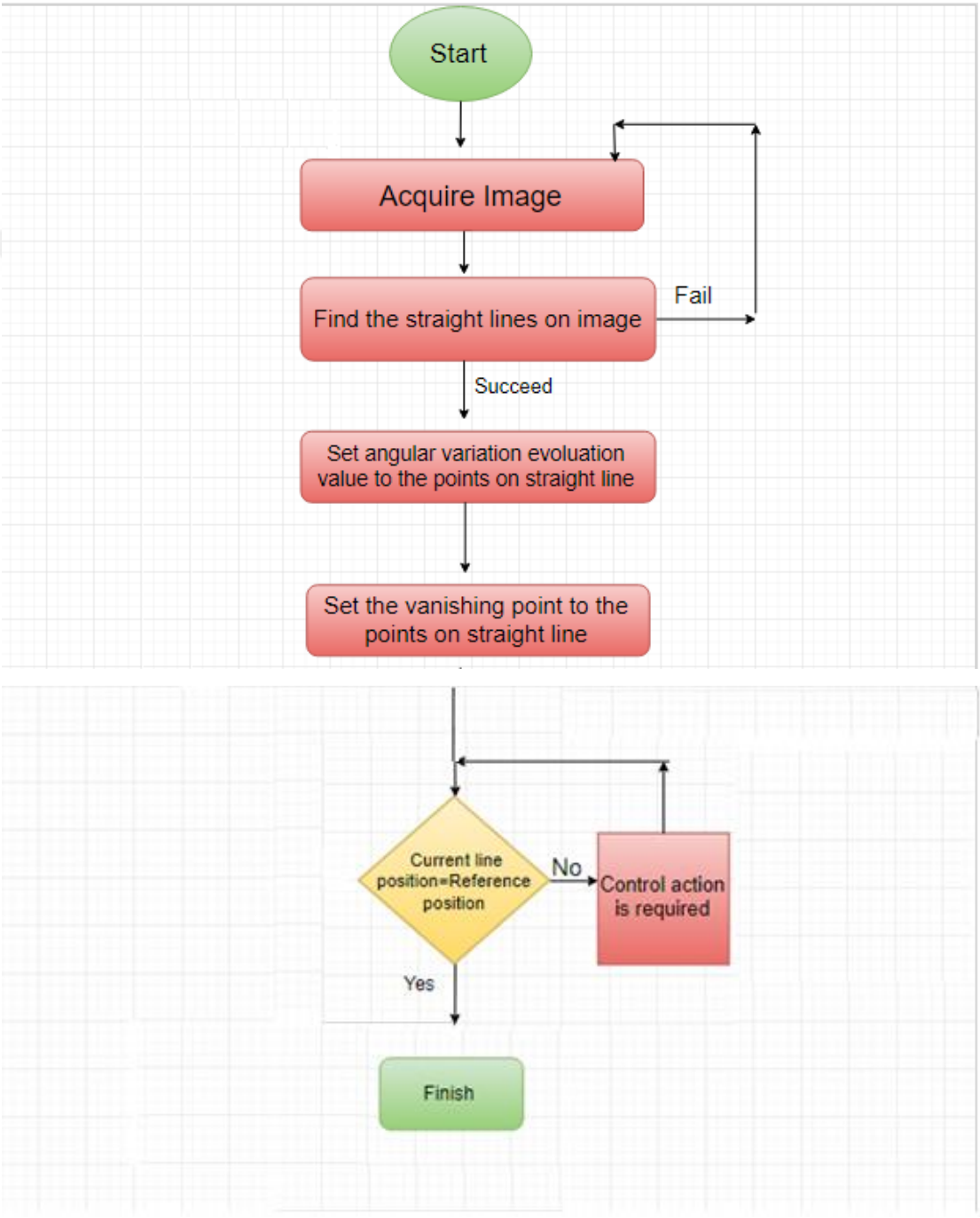

Figure 3.8 Flowchart of the system

3.4 Computer Simulation

The simulations are carried out in closed-loop with this block diagram structure, and the computer simulation model is presented in Figure 3.9 and 3.12 for the electrical and combined overall system models, respectively. Figure 3.1 provides a functional view of the DC motor of the wheelchair system, and Figure 3.9 and 3.12 represents the computer simulation model structure of the overall control system, which yields the results discussed in Chapter 4.

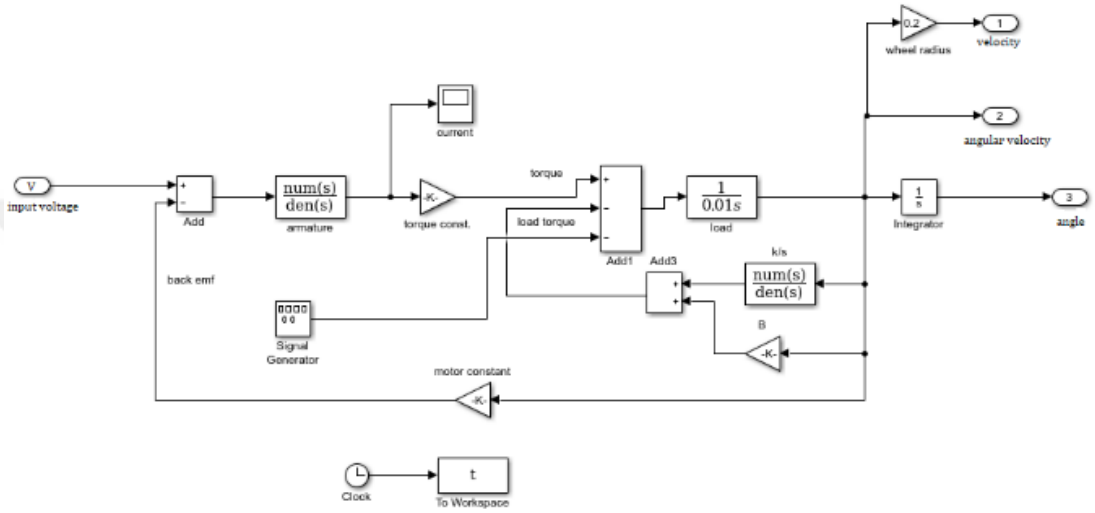

Figure 3.9 Computer simulation of DC motor of the wheelchair

When the computer simulation model which is presented in Figure 3.9 is examined, the equivalence of the parameters of block diagram is visible. For example, input voltage (V) represents $\boldsymbol{E_a}$, angular velocity represents $\boldsymbol{\omega}$, angle represents $\boldsymbol{\theta}$ etc. Additionally, we have added a signal generator in computer simulation to represent the disturbance effect on the system. Disturbance effect and results are shown in the following chapter. The values of system parameters which are presented in Table 3.1 are used in the computer simulation.

Table 3.1 Values of System Parameters

$\boldsymbol{E_a}$	24 V
$\boldsymbol{R_a}$	1.4 Ω
$\boldsymbol{L_a}$	0.5 H

$\boldsymbol{K_T}$	0.05 V/rad./sec.
$\boldsymbol{K_v}$	0.05 V/rad./sec.
$\boldsymbol{J_T}$	0.0166 kg.$\boldsymbol{m^2}$
B	0.02 (damping coeff.)
k	0.0001 N/m

When we closely examined the system in Figure 3.10, we observe the applied voltage (voltage 1) as one input and there are three outputs. Velocity 1 represents velocity of the right wheel of the wheelchair, angular speed 1 represents angular speed of the right wheel of the wheelchair and angle 1 represents linear displacement of the right wheel of the wheelchair. Figure 3.9 is the open form of Figure 3.10. Results of output responses are explained and graphivcally presented in Chapter 4. The wheelchair has two identical motors, so the simulation model for the right motor is used for the left motor at the same time. Responses to fluctuation of different voltages can be seen as an output velocity, angular speed and displacement.

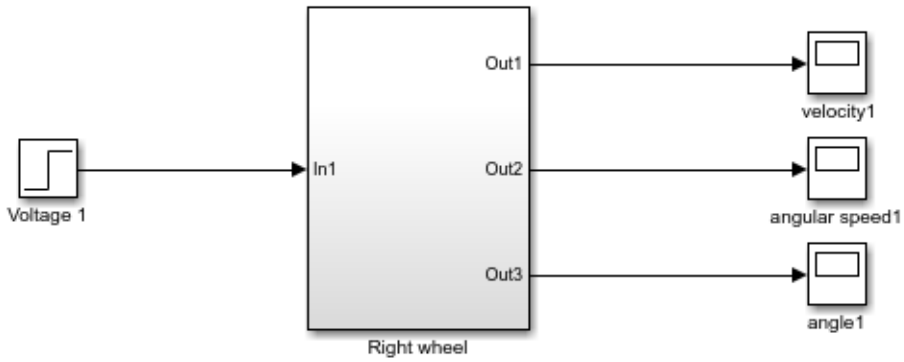

Figure 3.10 Computer simulation for one wheel

The function block which is shown in Figure 3.12 is constructed to observe the wheelchair body movement and orientation angle. Right wheel velocity, left wheel velocity, right wheel displacement, left wheel displacement and mass are used in this process. Also, rider mass effect is analyzed with this function. Results of the rider mass effect to body movement of wheelchair is shown in graphics in Chapter 4.

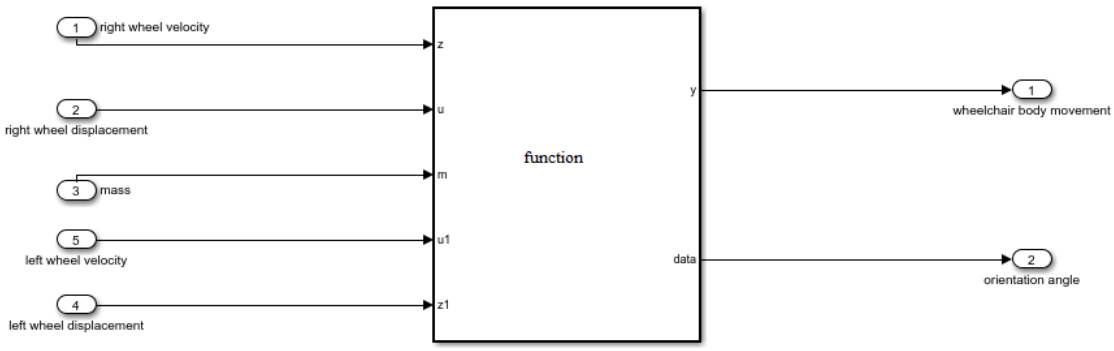

Figure 3.11 Function in the computer simulation

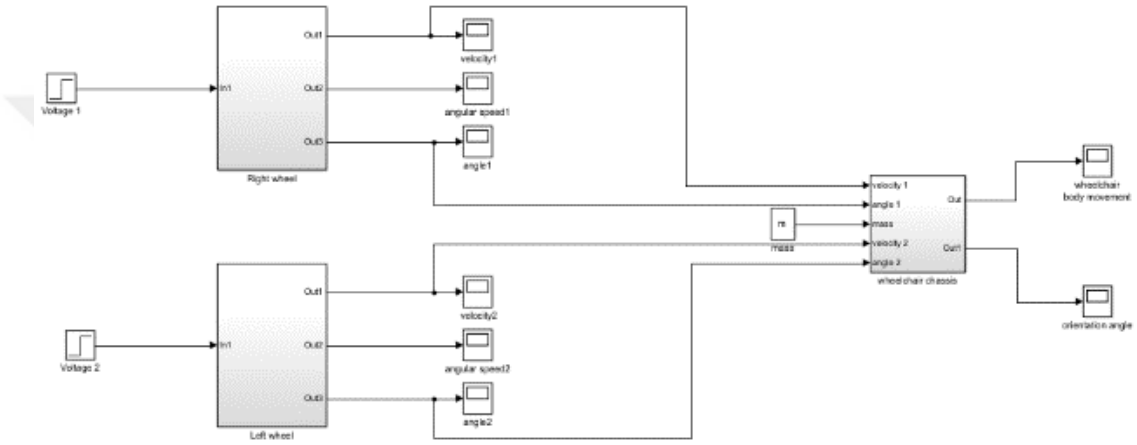

Figure 3.12 Computer simulation model of whole system

The autonomous wheelchair control system in the current study has two major parts. One of them is the image processing part that is supposed to generate visual feedback signal, and the other one is the motor control part that is supposed to implement motion control of the autonomous wheelchair using visual feedback. Driving the DC motor is provided with signal inputs which come from image processing data. Control of the wheelchair turning left or right is provided by different voltage levels applied to the motors. For example, when turning to right is planned with maximum rate, voltage 2 must have maximum voltage and voltage 1 must have zero voltage, and when turning to left is planned with maximum rate, voltage 1 must have maximum voltage and voltage 2 must have zero voltage. Also, this simulation gives the information about linear displacement and orientation angle of the wheelchair depending on the voltage applied. The simulation provides the possibility of changing parameters of the wheelchair, so the effective motion control system design in practice can be done easily with this simulation results.

CHAPTER 4

SIMULATION RESULTS

4.1 Introduction

After theoretical analysis of autonomous wheelchair and designing a simulation model for the system it is necessary to observe model performance. To do that, a computer simulation software package for modeling, simulating and analyzing dynamical systems is used. Feedback control system is verificationed with visual data which is collected from outdoor environment. When the computer simulation model which is shown in Figure 3.2 is executed, model performance can be seen in graphics.

4.2 Motion Control Tests

4.2.1 DC Motor Performance

In this section, the DC motor of the wheelchair is simulated with step input at peak voltage of 24 Volts for one motor. The figures show maximum displacement and velocities for one wheel (see Figures 4.1-4.3). In Figure 4.1, the graph shows (θ-t) linear displacement for one wheel in radians with respect to time in 10 seconds. Figure 4.2. presents the (ω-t) variation, and it shows that maximum angular velocity of ω=40 rad/s (which is equal to ω =8 m/s) is reached with respect to time in 10 seconds. Figure 4.3 shows that the (v-t) curve reached maximum linear velocity of v=1.6 m/s (which is equal to v=5.76 km/h) with respect to time in 10 seconds.

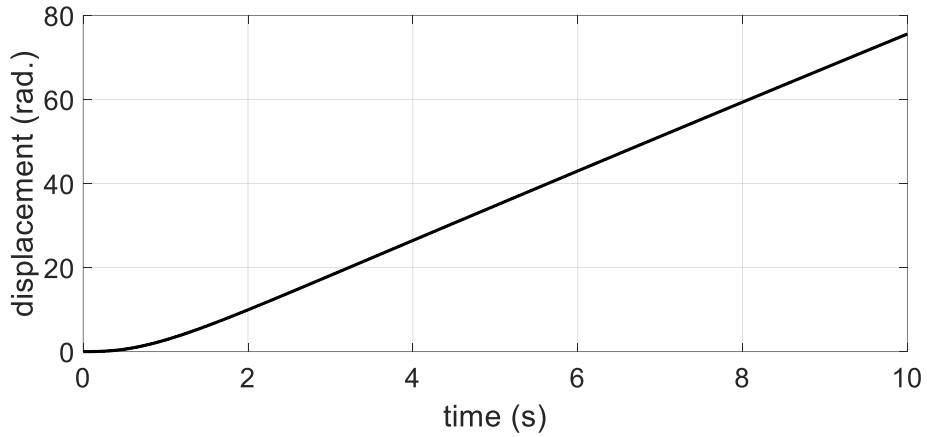

Figure 4.1 Linear displacement for one wheeel

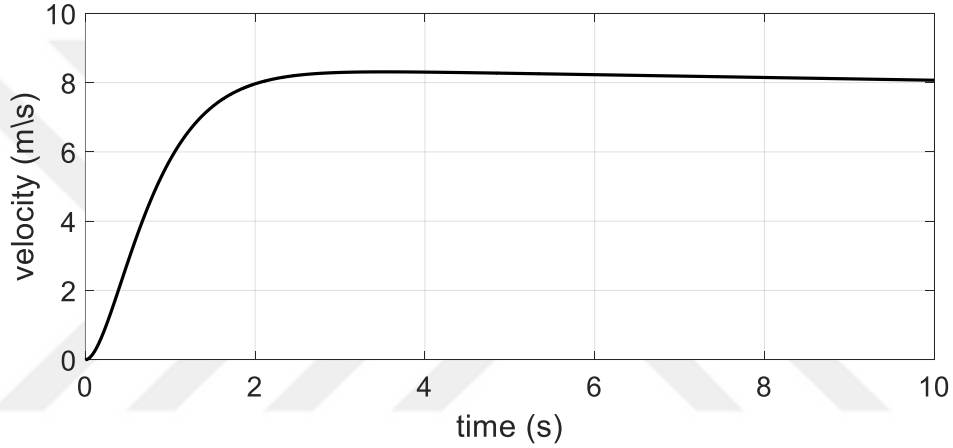

Figure 4.2 Angular velocity for one wheel

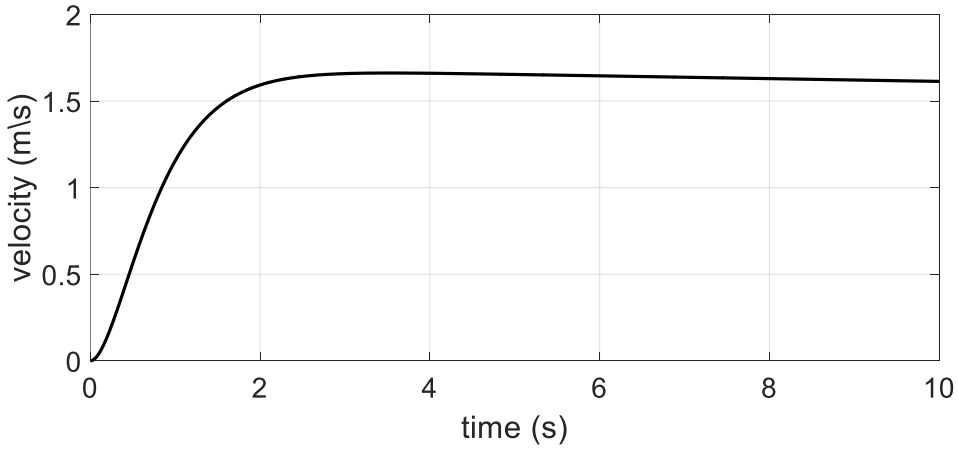

Figure 4.3 Linear velocity for one wheel

4.2.2 Disturbance and Rider Mass Tests

The results presented in Figures 4.4 and 4.5 are aimed to show the effectiveness of the motion control system combined with the PW dynamics to disturbance effects and rider mass tests. Parameter values of disturbances and rider masses are given in the Table 4.1. The graphs in Figure 4.4 show the effect of disturbances of different amplitudes on the velocity of the wheelchair. The graphs in Figure 4.5 show the effect of rider mass variations, where individuals with different weights are assumed to ride the wheelchair, and the wheelchair displacement results are presented.

Figures 4.6 and 4.7 present the simulation results where the wheelchair body motion and orientation angle are investigated. The graph in Figure 4.5 shows linear displacement of wheelchair body movement in forward direction in Radians. It reaches 141.70 Radians in 10 seconds. The graphs in Figure 4.6 show wheelchair's orientation angle when it turns clockwise and anticlockwise directions for 2 seconds.

Table 4.1 Parameters used in the simulation

Parameters	Parameter values
Rider mass 1	40 kg.
Rider mass 2	60 kg.
Rider mass 3	80 kg.
Rider mass 4	100 kg.
Disturbance amplitude 1	0.005
Disturbance amplitude 2	0.01
Disturbance amplitude 3	0.015
Disturbance amplitude 4	0.02

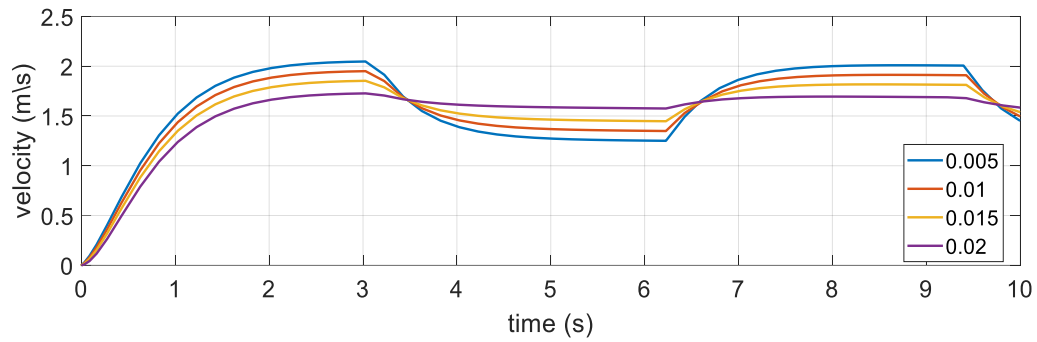

Figure 4.4 Disturbance effect

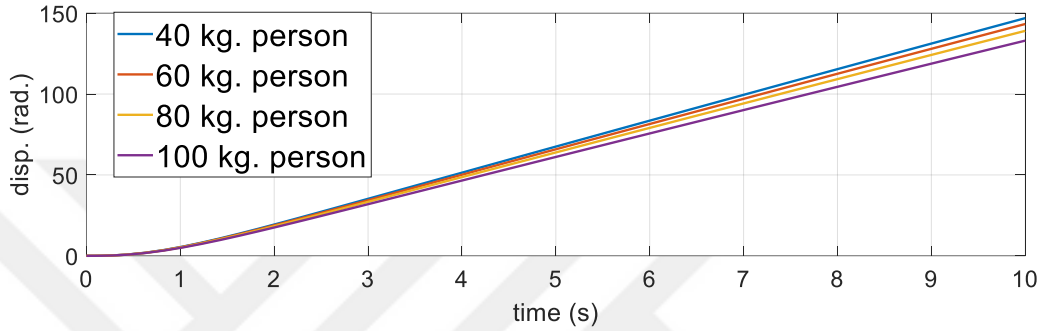

Figure 4.5 Effect of rider mass

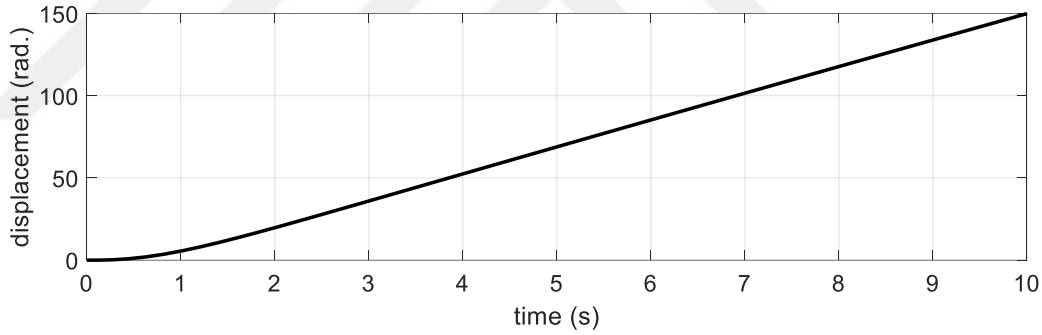

Figure 4.6 Wheelchair body movement in forward direction

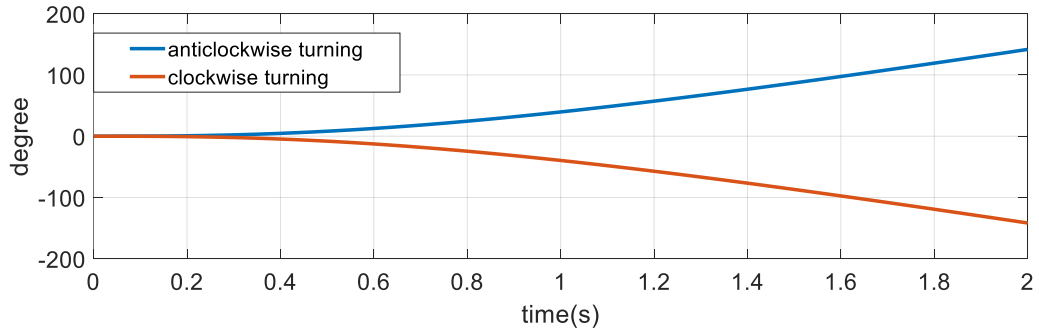

Figure 4.7 Wheelchair's orientation angle

The simulation results are consistent with expected movement of the wheelchair body, and the feedback control performance is revealed through simulations in closed-loop. The effect of disturbances and rider mass variations presented in simulation results are useful in future attempts for enhancing the robustness of the wheelchair motion control system. Control oriented simulation model proves itself as a useful tool for preliminary tests in design of the autonomous wheelchair navigation and control system using visual feedback signal.

4.3 Visual Feedback Control

Visual servo control relies on techniques from image processing and control theory. Image based servo control is the one of the major classification of systems on image processing. As mentioned before in the introduction part of the thesis, IBVS use the image plane coordinates of a set of points. And it can be seen path following in the wheelchair tracking. The path is defined as a set of intermediate images while the task of the IBVS controller is to drive the chair through places which are represented using these intermediate images. The task is designed to completion by proposing a visual controller that utilizes the well common IBVS along with robust features extraction methods to be used in the control law. These features are the vanishing point which is appeared due to straight lines in the urban environment, and the line of gravity of yellow color tactile path marker which will be robustly detected and tracked. There are 4 examples of images as can be seen in the Figure 4.8, 4.9, 4.10 and 4.11. Then, Figure 4.12, 4.13, 4.14 and 4.15 shows the vanishing point of this images. When we turn the camera to right, coordinate of vanishing point changes and control algorithm works for keeping the wheelchair on the line. Algoritm do this process by applying the voltage the wheel of the wheelchair which is needed. Also, this situation is valid for left side.

Figure 4.8 Image example 1

Figure 4.9 Image example 2

Figure 4.10 Image example 3

Figure 4.11 Image example 4

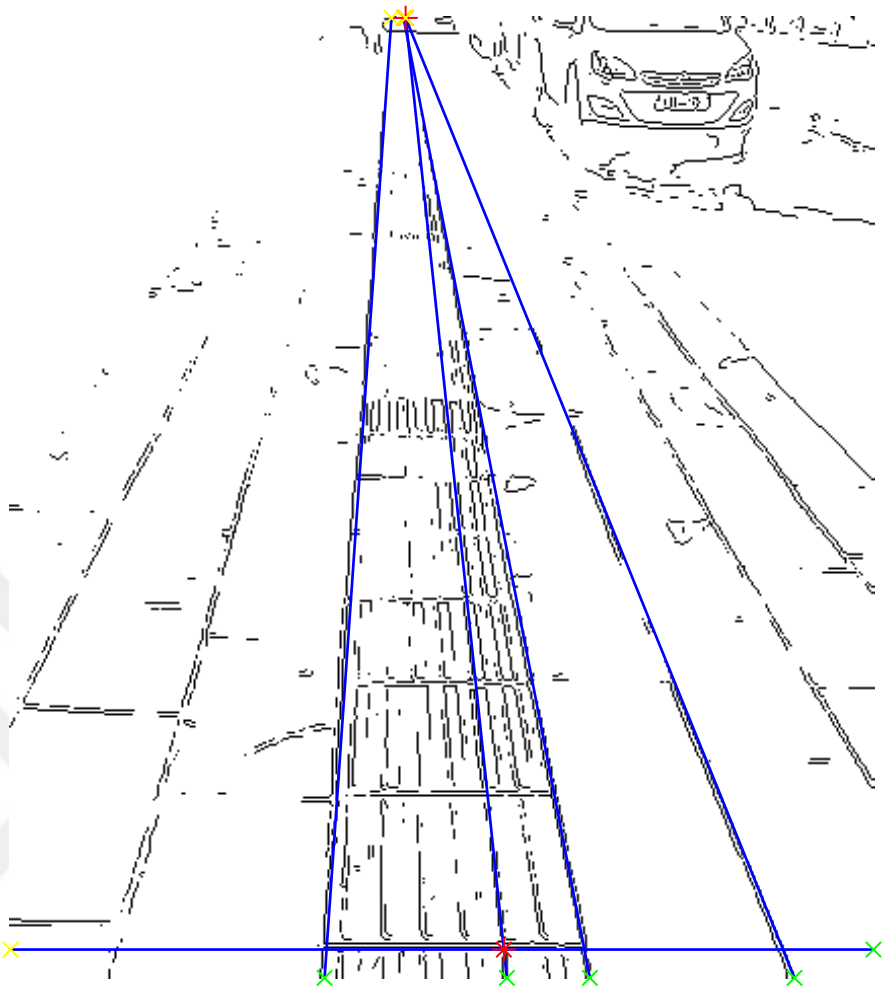

Figure 4.12 Vanishing point of first image

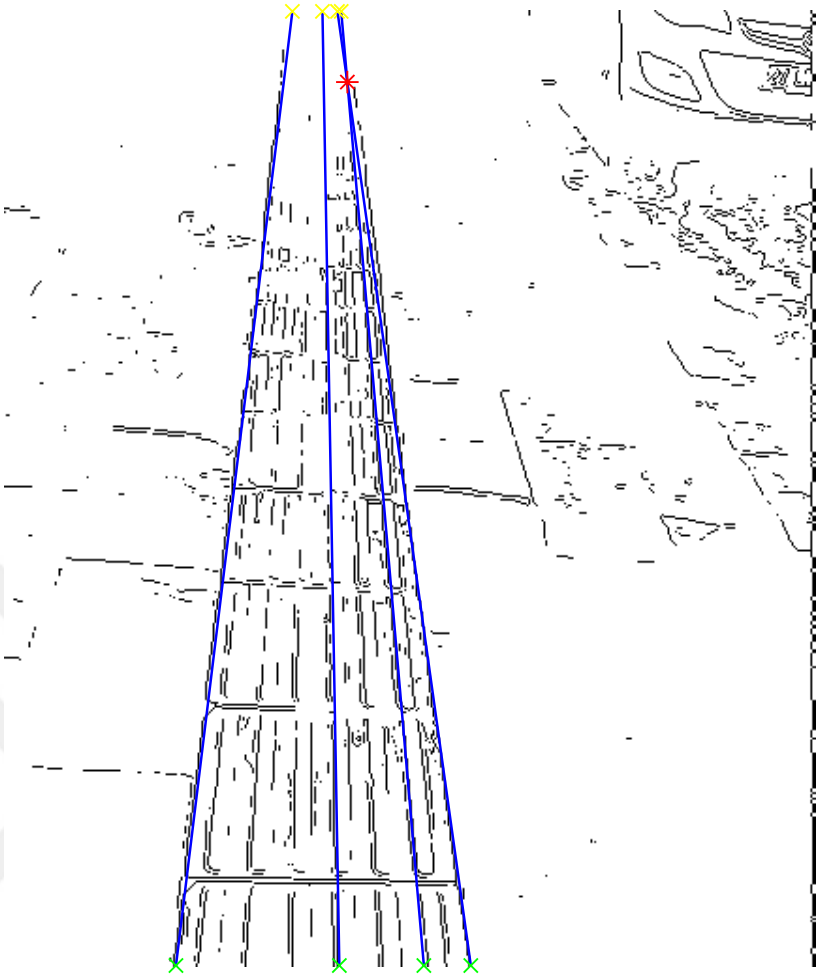

Figure 4.13 Vanishing point of second image

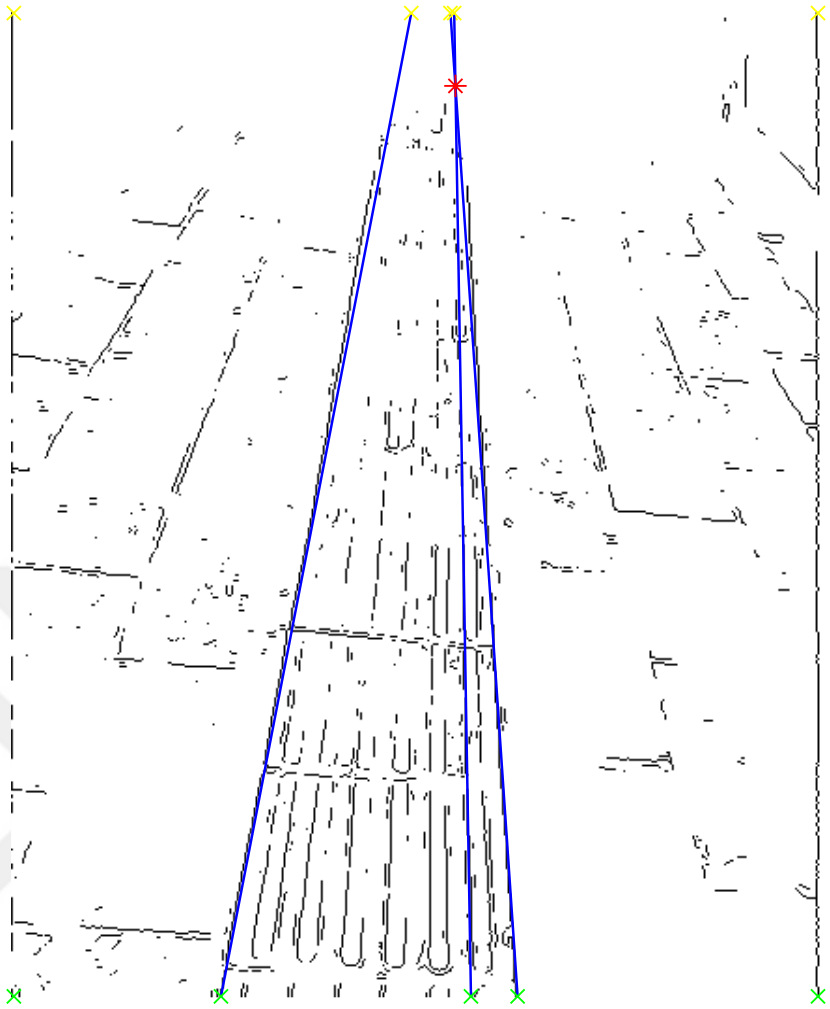

Figure 4.14 Vanishing point of third image

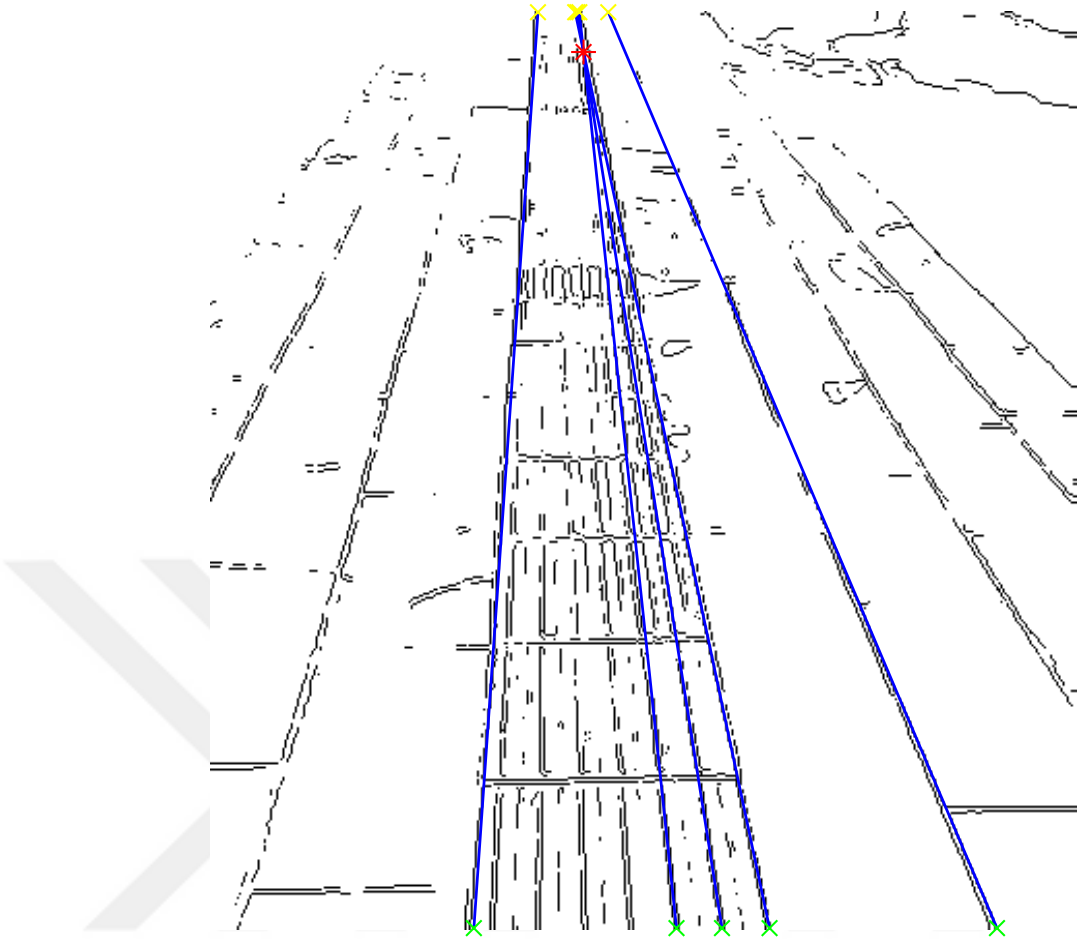

Figure 4.15 Vanishing point of fourth image

CHAPTER 5

CONCLUSIONS

5.1 Concluding Remarks

This thesis presents results of the study on dynamic modeling and computer simulation of an autonomous wheelchair with control purposes. The research consists of three main parts. Firstly, linear model of DC motor is extracted and analyzed for right and left wheels of the wheelchair. Secondly, mathematical model of the chassis of the wheelchair is obtained. Thirdly, integration with dynamic model of DC motor is completed by using system parameters.

Using the results of simulation tests, control algorithm is developed for efficient motor control. Linear displacement, position control, direction control and velocity of wheelchair are presented in the computer simulation results. Also, effect of disturbances and effect of rider mass are shown in the figures. It is revealed that obtained mathematical model is capable of representing autonomous wheelchair dynamics in open-loop and closed-loop and simulation results prove effectiveness of the model and designed control system.

Motion control and tracking via visual feedback is also achieved using a feedback control system with visual data collected from outdoor environment. Simulation tests for visual feedback is done by using images. The results show that the designed control algorithm provides effective control motion of the autonomous wheelchair.

5.2 Future Work and Recommendations

Results of the study will be used in the research project that aims to solve the autonomous wheelchair control problem. This work constitutes an important part of the project. Real control system design will be constructed to the results of this simulation. After entegrating the image processing methods which is proposed in the first chapter, the project will solve the outdoor navigation problem by using only vision sensor.

REFERENCES

[1] Vysotska, O., Naseer, T., Spinello, L., Burgard, W., & Stachniss, C. (2015). Efficient and effective matching of image sequences under substantial appearance changes exploiting GPS priors. *IEEE International Conference on Robotics and Automation* , 2774–2779.

[2] Wyeth, G., & Milford, M. (2011). Towards lifelong navigation and mapping in an office environment. In *Springer Tracts in Advanced Robotics* ,**70**, 589–603.

[3] A. H. Abdul Hafez, Manpreet Arora, K. Madhava Krishna & C. V. Jawahar (2016) Learning multiple experiences useful visual features for active maps localization in crowded environments, *Advanced Robotics*, **30(1)**, 50-67.

[4] Boubou, S., Hafez, A. H. A., & Suzuki, E. (2015). Visual impression localization of autonomous robots. In *IEEE International Conference on Automation Science and Engineering* **,** 328–334.

[5] Arroyo, R., Alcantarilla, P. F., Bergasa, L. M., & Romera, E. (2015). Towards life-long visual localization using an efficient matching of binary sequences from images. In *Proceedings - IEEE International Conference on Robotics and Automation* **,** 6328–6335.

[6] Diosi, A., Šegvić, S., Remazeilles, A., & Chaumette, F. (2011). Experimental evaluation of autonomous driving based on visual memory and image-based visual servoing. *IEEE Transactions on Intelligent Transportation Systems*, ***12*(3)**, 870–883.

[7] Cherubini, A., & Chaumette, F. (2013). Visual navigation of a mobile robot with laser-based collision avoidance. *International Journal of Robotics Research*, ***32*(2)**, 189–205.

[8] Courbon, J., Mezouar, Y., Lequievre, L., & Eck, L. (2008). Navigation of urban vehicle: An efficient visual memory management for large scale environments. In *2008 IEEE/RSJ International Conference on Intelligent Robots and Systems, IROS* 1817–1822.

[9] Abdul Hafez, A. H., Cervera, E., & Jawahar, C. V. (2013). Stable hybrid visual servo control by a weighted combination of image-based and position-based algorithms. *International Journal of Control and Automation*, ***6*(3),** 149–164.

[10] Badino, H., Huber, D., & Kanade, T. (2012). Real-time topometric localization. In *Proceedings - IEEE International Conference on Robotics and Automation* 1635– 1642.

[11] Zisserman, A., & Hartley, R. I. (2004). *Multiple View Geometry*. *IEEE Transactions on Pattern Analysis and Machine Intelligence*, **25**.

[12] E. Lutton, H. Maitre, J. Lopez-Krahe, (1994). "Contribution to the determination of vanishing points using Hough transform", *Pattern Analysis and Machine Intelligence IEEE Transactions*, **16**, 430-438.

[13] Straforini, M., Coelho, C., & Campani, M. (1993). Extraction of vanishing points from images of indoor and outdoor scenes. *Image and Vision Computing*, ***11*(2),** 91–99.

[14] Aguilera, A., Menéndez, S. G. L., & Pérez-Aguila, R. (2005). A procedure for comparing color 2-dimensional images through their extrusions to the 5-dimensional colorspace. In *Proceedings - 15th International Conference on Electronics, Communications and Computers*, 300–305.

[15] He, B. W., & Li, Y. F. (2007). A novel method for camera calibration using vanishing points. In *Proceedings 14th International Conference on Mechatronics and Machine Vision in Practice, M2VIP2007* , 44–47.

[16] Tardif, J. P. (2009). Non-iterative approach for fast and accurate vanishing point detection. In *Proceedings of the IEEE International Conference on Computer Vision* , 1250–1257.

[17] Kessler, C., Ascher, C., Frietsch, N., Weinmann, M., & Trommer, G. F. (2010). Vision-based attitude estimation for indoor navigation using vanishing points and lines. In *Record - IEEE PLANS, Position Location and Navigation Symposium* 310–318.

[18] Grater, J., Schwarze, T., & Lauer, M. (2015). Robust scale estimation for monocular visual odometry using structure from motion and vanishing points. In *IEEE Intelligent Vehicles Symposium, Proceedings* , 475– 480.

[19] Zhang, G., Kang, D. H., & Suh, I. H. (2012). Loop closure through vanishing points in a line-based monocular SLAM. In *Proceedings - IEEE International Conference on Robotics and Automation*, 4565–4570.

[20] Ebrahimpour, R., Rasoolinezhad, R., Hajiabolhasani, Z., & Ebrahimi, M. (2012). Vanishing point detection in corridors: using Hough transform and K-means clustering. *IET Computer Vision*, ***6*(1),** 40.

[21] Schuster, R., Ansari, N., & Bani-Hashemi, A. (1993). Steering a Robot with Vanishing Points. *IEEE Transactions on Robotics and Automation*, ***9*(4),** 491–498.

[22] Simpson, R. C., & Levine, S. P. (1999). Automatic adaptation in the NavChair Assistive Wheelchair Navigation System. *IEEE Transactions on Rehabilitation Engineering : A Publication of the IEEE Engineering in Medicine and Biology Society*, ***7*(4),** 452–463.

[23] Vander Poorten, E. B., Demeester, E., Reekmans, E., Philips, J., Hüntemann, A., & De Schutter, J. (2012). Powered wheelchair navigation assistance through kinematically correct environmental haptic feedback. In *Proceedings - IEEE International Conference on Robotics and Automation* 3706–3712.

[24] Sert, H., Perruquetti, W., Kokosy, A., Jin, X., & Palos, J. (2012). Localizability of unicycle mobiles robots: An algebraic point of view. In *IEEE International Conference on Intelligent Robots and Systems* , 223–228.

[25] Deshpande, N., Grant, E., & Henderson, T. C. (2014). Target localization and autonomous navigation using wireless sensor networks - A pseudogradient algorithm approach. *IEEE Systems Journal*, ***8*(1),** 93–103.

[26] Yayan, U., Akar, B., Inan, F., & Yazici, A. (2014). Development of indoor navigation software for intelligent wheelchair. - *Institute of Electrical and Electronics Engineers International Symposium on Innovations in Intelligent Systems and Applications* , 325–329.

[27] Schwesinger, D., & Spletzer, J. (2016). A 3D approach to infrastructure-free localization in large scale warehouse environments. In *IEEE International Conference on Automation Science and Engineering* , 274–279.

[28] Secchi, H., Carelli, R., & Mut, V. (2003). An experience on stable control of mobile robots. *In Latin American Applied Research* , **33**, 379–385.

[29] Carelli, R., Soria, C., Nasisi, O., & Freire, E. (2002). Stable AGV corridor navigation with fused vision-based control signals. In *IECON Proceedings (Industrial Electronics Conference)* , **3,** 2433–2438.

[30] Chung, W., Kim, S., Choi, M., Choi, J., Kim, H., Moon, C. B., & Song, J. B. (2009). Safe navigation of a mobile robot considering visibility of environment. *IEEE Transactions on Industrial Electronics*, ***56*(10),** 3941–3950.

[31] Yuan L. (2013) Ubiquitous Visual Navigation for the Robotic Wheelchair. In: Sun Z., Deng Z. (eds) *Proceedings of 2013 Chinese Intelligent Automation Conference. Lecture Notes in Electrical Engineering*, **255**, 103-110.

[32] Gillham, M., Howells, G., & Kelly, S. (2016). Assistive Trajectories for Human-in-the-Loop Mobile Robotic Platforms. In *Proceedings - 2015 6th International Conference on Emerging Security Technologies, EST 2015,* 56–61.

[33] Babel, M., Pasteau, F., Guégan, S., Gallien, P., Nicolas, B., Fraudet, B., … Guillard, D. (2016). HandiViz project: Clinical validation of a driving assistance for electrical wheelchair. In *Proceedings of IEEE Workshop on Advanced Robotics and its Social Impacts, ARSO* .

[34] Devigne, L., Narayanan, V. K., Pasteau, F., & Babel, M. (2016). Low complex sensor-based shared control for power wheelchair navigation. In *IEEE International Conference on Intelligent Robots and Systems* , 5434–5439.

[35] Langelaan, J. W., Spletzer, J., Montella, C., & Grenestedt, J. (2012). Wind field estimation for autonomous dynamic soaring. In *Proceedings – IEEE International Conference on Robotics and Automation* , 16–22.

[36] Filliat, D., & Meyer, J. A. (2002). Global localization and topological map-learning for robot navigation. In *Proceedings of the Seventh International Conference on Simulation of Adaptive Behavior (SAB 2002)* , 131–140.

[37] Johnson, B. W., & Aylor, J. H. (1985). Dynamic Modeling of an Electric Wheelchair. *Institute of Electrical and Electronics Engineers Transactions on Industry Applications*, IA-**21(5)**, 1284–1293.

[38] Park, J. J., Lee, S., & Kuipers, B. (2017). Discrete-time dynamic modeling and calibration of differential-drive mobile robots with friction. In Proceedings - *Institute of Electrical and Electronics Engineers International Conference on Robotics and Automation* , 6510–6517.

[39] Ogata, K. (2010). Modern Control Engineering, Prentice Hall, fifth edition, New Jersey, United States of America.

[40] Gocmen, A. Design of Two Wheeled Electric Vehicle, Master Thesis, Atılım University, Ankara.

[41] Jamil, O., Jamil, M., Ayaz, Y., & Ahmad, K. (2014). Modeling, control of a two-wheeled self-balancing robot. International Conference on Robotics and Emerging Allied Technologies in Engineering, – *Proceedings* . *Institute of Electrical and Electronics EngineersComputer Society*,191-199.

[42] Gupta, S., & Mazumdar, S.G. (2013). Sobel Edge Detection Algorithm. *International Journal of Computer Science and Management Research*, **2**, 1578-1583.

[43] Sobel Edge Detector.Available at: https://homepages.inf.ed.ac.uk/rbf/HIPR2/sobel.htm, Accessed:06.11.2018.